

# Experimental Determination of Frictional Interface Models

Matthew S. Bonney  
 University of Wisconsin-Madison  
 Madison, WI, USA  
[msbonney@wisc.edu](mailto:msbonney@wisc.edu)

Brett A. Robertson  
 Arizona State University  
 Tempe, AZ, USA  
[baroher@sandia.gov](mailto:baroher@sandia.gov)

Fabian Schempp  
 University of Stuttgart  
 Stuttgart, Germany  
[fabian.schempp@gmx.de](mailto:fabian.schempp@gmx.de)

Marc Mignolet  
 Arizona State University  
 Tempe, AZ, USA  
[marc.mignolet@asu.edu](mailto:marc.mignolet@asu.edu)

Matthew R. Brake  
 Sandia National Labs  
 Albuquerque, NM, USA  
[mrbrake@sandia.gov](mailto:mrbrake@sandia.gov)

October 26, 2015

## Abstract

The focus of this paper is on continuing the experimental/modeling investigation of the Brake-Reuß beam which was initiated a year ago as part of the NOMAD program at Sandia National Labs. The ultimate goal of the overall effort is to (i) determine the parameters of joint models, in particular the Iwan model in its modal form, from well delineated tests and (ii) extend this approach to identify statistical distributions of the model parameters to account for joint uncertainty. The present effort focused on free response of the the beam resulting from an impact test. The use of this data in conjunction with the Hilbert transform is shown to provide a straightforward framework for the identification of the joint model parameters at the contrary of the forced response data used earlier. The resulting frequency and damping vs. amplitude curves are particularly conducive to a Iwan-type modeling which is demonstrated. There curves also show the effect of the bolt torque on the joint behavior, i.e., increase in natural frequency, linear limit, and macroslip threshold. Macroslip is shown to have occurred in some of the tests and it is concluded from ensuing testing that this event changed the nature of the jointed beams. Specifically, the linear natural frequency (observed under very low level impact test) shifted permanently by 20Hz and, in one case, the linear natural frequency was observed to decrease with increasing bolt torque level in opposition to other beams and physical expectations. An analysis of the joint surface strongly suggest that a significant plastic zone developed during the macroslip phase which induced the above unusual behaviors.

# 1 Introduction and Background

The prediction of the dynamic response of assembled structures is of particular importance in many different areas such as the automotive, aerospace, and nuclear weapons areas. The characterization of joints, most notably their complex nonlinear behavior and variability, represents one of the most significant challenges in achieving the desired accuracy of predictions [7]. Accordingly, the dynamics of joints has been an important research topic for many years with many significant results obtained. Yet, there is still need for additional work, in particular for the gathering and analysis of experimental data on simple configuration(s) to support the modeling effort of both deterministic and uncertain joint models. Such an effort was initiated last year under the framework of the NOMAD program at Sandia National Labs [6]. The present investigation is the continuation of these efforts.

The reported work focuses on the Brake-Reuß beam which is a squared cross-section long beam exhibiting a 3-bolt lap joint at its middle. It is desired first to define a clear and comprehensive test protocol for this beam addressing the questions of free response or forced excitation, excitation level, bolt torque control, surface condition, etc. Next, the potential determination of the parameters of proposed joint models is investigated using such techniques as the Hilbert transform. The variability of the parameters of these joint models is a third component of this global effort.

The contributions of this paper within the multi-year effort described above focused more specifically on assessing the potential use of free response data and proposing a corresponding preliminary test protocol. The use of the Hilbert transform of this free response data to support the identification of the parameters of an Iwan model is also assessed.

## 2 Proposed Joint Models

Several different models have been created to represent joints in structures [3]. A few that are commonly used are the Coulomb Friction model, the Jenkins Element, and the Iwan Element. Each of these has a different way of simulating the friction and dissipation across a joint. Coulomb friction and the Jenkins element are discrete models while the Iwan element [8] is a more distributive one. Although they all are based on friction between two surfaces, the parameters that characterize each model are different and therefore must be obtained separately. The coefficient of friction can be found using a Coulomb friction and wear experiment while other parameters must be found using response data from say modal impact hammer tests. More details of each model and their parameters are described in the following sections.

### 2.1 Coulomb Friction

The Coulomb Friction model takes into account basic sliding contact friction and is depicted as in Fig. 1. The only parameter present in this model is the coefficient of friction, which for a given surface can be measured experimentally as discussed in more detail in the Experimentation section.

Modeling a joint using Coulomb friction leads to energy dissipation when the two surfaces slide on each other. However, unlike the more complex joint models, it does not allow microslip at the interface to occur; it only accounts for the entire surface sliding, i.e., macroslip. Note that the capability to slip provides new deformation possibilities and thus lowers the natural frequencies. A physical interpretation of a Coulomb friction slider and its forces is shown in

### 2.2 Jenkins Element

The Jenkins element [4], see Fig. 2, is a spring-slider combination that can be in one of two states: stick or slip. If the slider is stuck, there is no friction or energy dissipation and only the linear spring is active. Once the force in the spring reaches the static friction threshold, the slider will then slip causing friction to become active and the spring force to stay constant. The Jenkins model allows for linear and nonlinear deformations

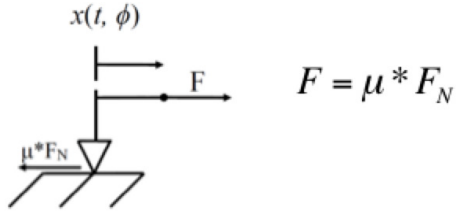


Figure 1: Coulomb Friction Model

in the joint at the contrary of the Coulomb friction which does not exhibit linear deformations. However, the Jenkins element only allows for the entire joint to slip, so the joint can exhibit macroslip but not microslip. The model parameters for a Jenkins element are the coefficient of friction and the spring coefficient.

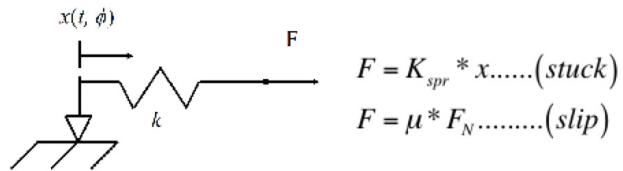


Figure 2: Jenkins Model

### 2.3 Iwan Element

The Iwan element is a more complex joint model involving multiple Jenkins elements connected in parallel, see Fig. 3 [8]. Specifically, assuming a continuous distribution of them, the total force in the element corresponding to a displacement  $x$  [8] is

$$F(t) = \int_0^\infty \rho(\phi)(u(t) - x(t, \phi))d\phi, \quad (1)$$

where the distribution of sliders,  $\rho$ , is given by

$$\rho(\phi) = R\phi^\chi[H(\phi) - H(\phi - \phi_{max})] + S\delta(\phi - \phi_{max}) \quad (2)$$

for the particular case of the 4-parameter model [8]. In the above equation,  $H$  is the Heavyside (step) function while  $R$ ,  $\chi$ ,  $\phi_{max}$ , and  $S$  are the parameters of the model. The latter two specify the macroslip limit  $\phi = \phi_{max}$  with  $S$  denoting the number of sliders slipping at that level. The parameters  $R$ ,  $\phi_{max}$ , and  $S$  are usually converted to another set of more physical parameters that can be determined experimentally. They are  $F_s$ ,  $K_T$ , and  $\beta$  (see [8] for relations). Specifically,  $F_s$  is the force at which macroslip occurs and  $K_T$  is the interface stiffness of the joint. Note that  $\chi$  characterizes the change in energy dissipation vs. amplitude.

Unlike the single Jenkins element, a microslip region is possible for the Iwan model as each of the sliders has a different threshold at which it transitions from stick to slip. From that standpoint, it is a more desirable phenomenological representation of a joint because microslip is a important phenomenon of jointed interfaces.

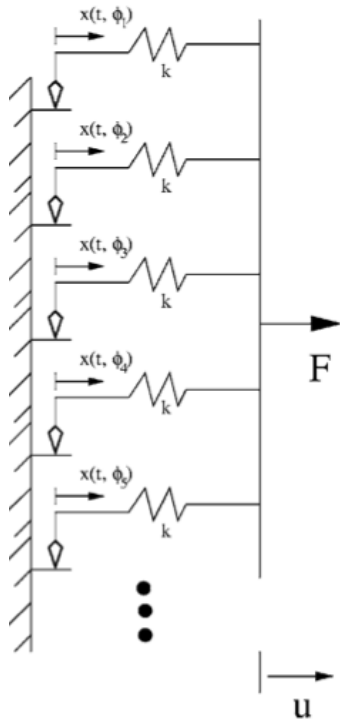


Figure 3: Iwan Model

### 3 Experimentation

The main objective of the present effort was to collect a large data set that can be used by other researchers for the development of uncertainty quantification techniques. This data is available to anyone by request to the authors. During the course of this research, three different experimental set-ups were used to (i) determine the Iwan model properties, (ii) determine the friction coefficients, and (iii) measure the interface profile. Each of these tests is explained separately below.

The test article is the Brake-Reuß beam, a computer rendering of which is shown in Fig. 4. The beam consists of two half beams that are cut from a solid beam. These two half beams are connected by three bolts in a lap joint. The model below shows the bolt holes but does not show the holes that are drilled to be attached to a mechanical shaker.

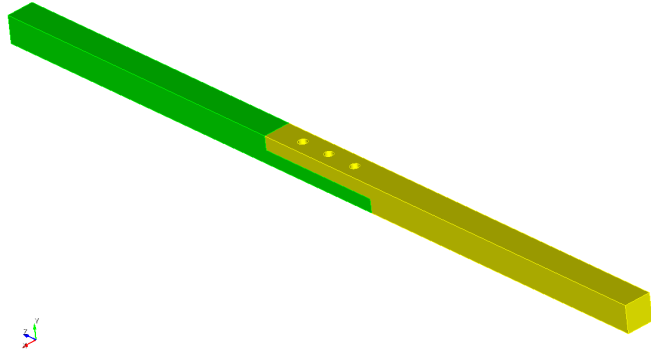


Figure 4: The Brake-Reuß Beam

During the testing, a total of six different beams with three different interface surface conditions were used. The first surface condition is the one resulting from the wire cutting procedure, i.e., without any polishing, beams 1&2. The other surfaces have prescribed surface conditions with mean asperity heights of  $0.8\mu\text{m}$  for beams 5&6, and  $1.6 - 3.2\mu\text{m}$  for beams 3&4. These heights are measured as described in the profiling testing section to verify the manufacturing process.

### 3.1 Impact Hammer Testing

The first experiment on this system consists in dynamic impact tests. The impulsive impact force from a hammer is recorded by its load cell and records of acceleration time histories are obtained from the accelerometers mounted on the beam. These time histories are first used to compute the corresponding frequency response function (FRF) for each accelerometer direction and then post-processed to determine the non-linear characteristics of the system, see section 4.

#### 3.1.1 Experimental Setup

The experimental setup for this test can be seen in Fig. 5. The beam is supported near its ends by bungee cords connected to a fixture to emulate a free-free condition [9]. The bolts were torqued to several different values, 3, 5, 7, 10, and  $15\text{Nm}$ , to assess the effect of this preload on the joint behavior. As will be seen, these values lead to a broad range of the first linear natural frequency of the beam which becomes saturated at the higher torque levels.

The magnitude of the impact was also varied leading to maximum input force approximately equal to 100, 8000 to 1000, 2000, 4000, and  $8000\text{N}$ . Note that the impact duration was around  $1\text{ms}$ . For impacts with maximum force larger or equal to  $2000\text{N}$ , the beam was thereafter retested at  $100\text{N}$  to assess whether any permanent deformation occurred during the high impact. Note that beams 1&5 were the only two impacted at levels leaving to 4000 and  $8000\text{N}$  maximum forces.

The beams were tested in its two transverse directions denoted as the Z for direction aligned with the axis of the bolt and Y as the direction along the width of the beam. Two accelerometers were used to capture the response of the beam, they were placed equidistantly from the center of the beam, outside of the joint zone.

#### 3.1.2 Test Data and Preliminary Analysis

Two types of data are collected during the testing: time history and frequency response. The time history is primarily used to identify the joint model parameters as explained in section 4. The frequency response is used to diagnose any problems in the testing.

For reference in the ensuing discussion, it was first desired to assess the effects of (i) surface finish, (ii) torque level, and (iii) impact level on the linear natural frequencies of the beams.

The effects of surface finish were first considered. It was expected that the linear natural frequency would increase as the surface becomes more smooth because there is more surface area in contact which allows for more stiffness in the interface and increases the natural frequency. The linear natural frequencies obtained with an impact level of  $100\text{N}$  and torque level of  $3\text{Nm}$  can be seen in Fig. 6. The above expectation is seen to hold overall with beams 1 and 2 of lower frequency than 3, itself of lower frequency than beams 5 and 6. Note the anomalous behavior of beam 4 which has the lowest natural frequency by a substantial amount, around  $15\text{Hz}$  lower. The reasons for this shift are not known but it is surmised that high impact ( $12,000\text{N}$  peak force) pre-testing experimentation generated large residual stresses. The occurrence of such stresses as a result of high impacts is discussed in section 5.

Consider next the changes in natural frequency with varying torque level. As it increases, it is expected that the natural frequency would increase as well as the resulting higher pressure at the interface increases the surface contact area. In turn, an increase in surface contact area increases the stiffness of the interface and

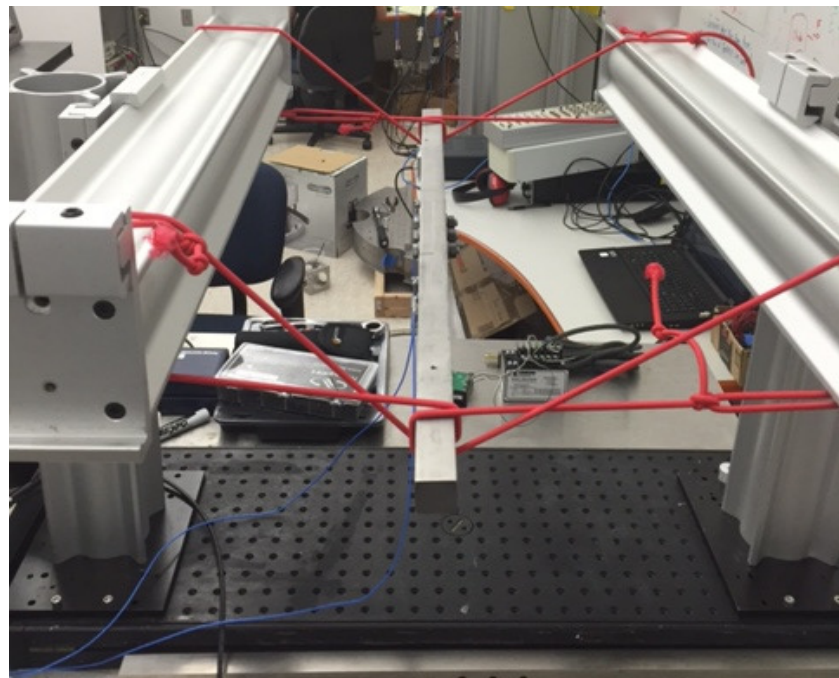


Figure 5: Experimental Setup

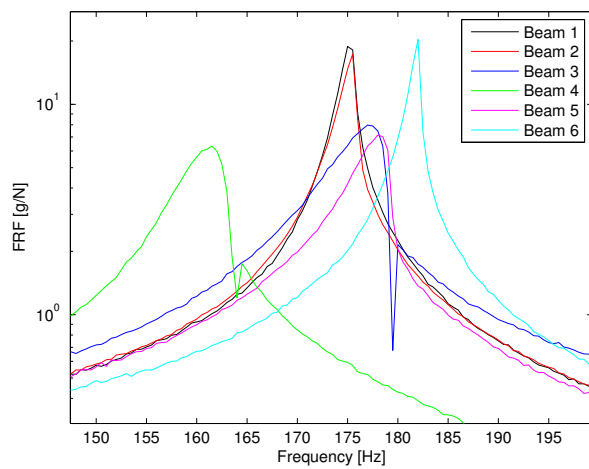


Figure 6: Linear Fundamental Frequencies of the 6 Different Beams

consequently the natural frequency. This increase can be seen in Fig. 7.

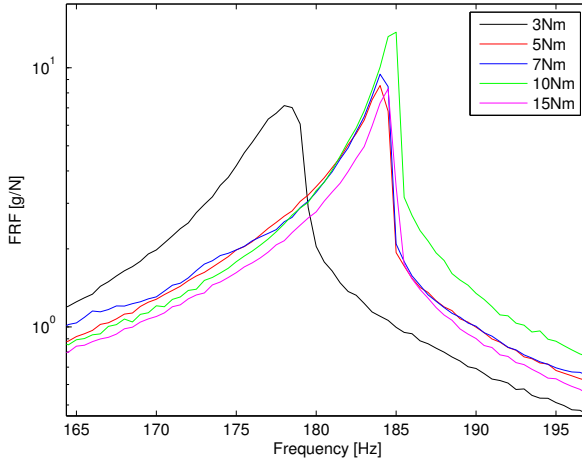


Figure 7: Fundamental Frequency of Beam 5 as a Function of Bolt Torque

Finally, the change in identified natural frequency resulting from an increase in impact force level is assessed. Prior testing of the Brake-Reuß beam [1] showed this beam to have a softening non-linearity. Thus, an increase with impact force level should result in a decrease in natural frequency. This was indeed the observed behavior, see Fig. 8.

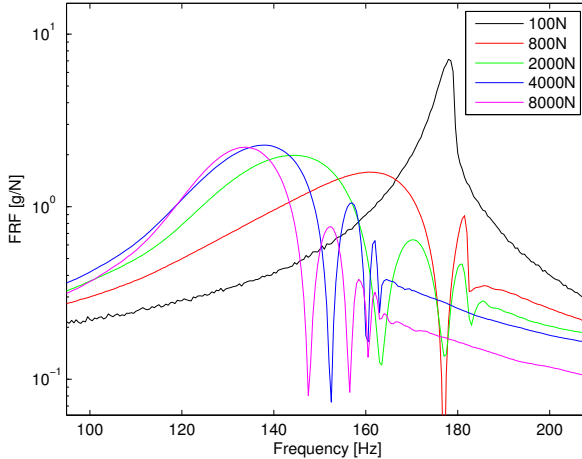


Figure 8: Beam 5 Fundamental Frequency as a Function of Maximum Input Force

### 3.2 Profile Testing

A wide variety of factors can influence the dynamic behavior of a joint and have consequently an effect on the parameters deduced for a numerical joint model. Such a factor could be the condition of the beam surface at the interface. Hence, to detect a possible correlation between the surface condition and the joint model parameters, profilometer data is collected and compared for all the different joint interfaces.

### 3.2.1 Experimental Setup

A Veeco Dektak 150 profilometer is used to carry out the tests. The data is collected by a stationary stylus that has a radius of  $12.5\mu\text{m}$  and senses the surface with a resolution of  $2\mu\text{m}/\text{sample}$ . To measure the surface condition on the lines depicted in Fig. 9, the beam is clamped on a movable disk.

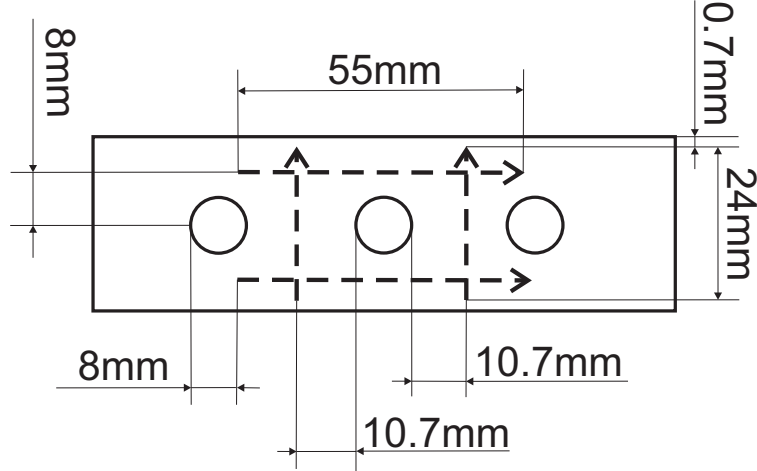


Figure 9: Positions of the measurements on the surface.

### 3.2.2 Reasoning

The six tested beams can be subdivided into three groups by the treatment of their interface surface. An untreated surface and two increments of polishing. For each of the three groups there are four half beams. The data from all beams are evaluated for roughness and waviness. For beams with different surface treatments, a substantial difference in roughness is expected, whereas the waviness should be fairly similar over all samples.

### 3.2.3 Test Data

Due to the mechanics of the disk and the clamping procedure, the surface is not exactly level when clamped on the disk of the profilometer during the measurement. The data is corrected for this in the first postprocessing step. From this raw data the roughness and waviness of the surfaces of each beam are then deduced. The roughness and waviness of all beams can be seen in Figs. 10-15

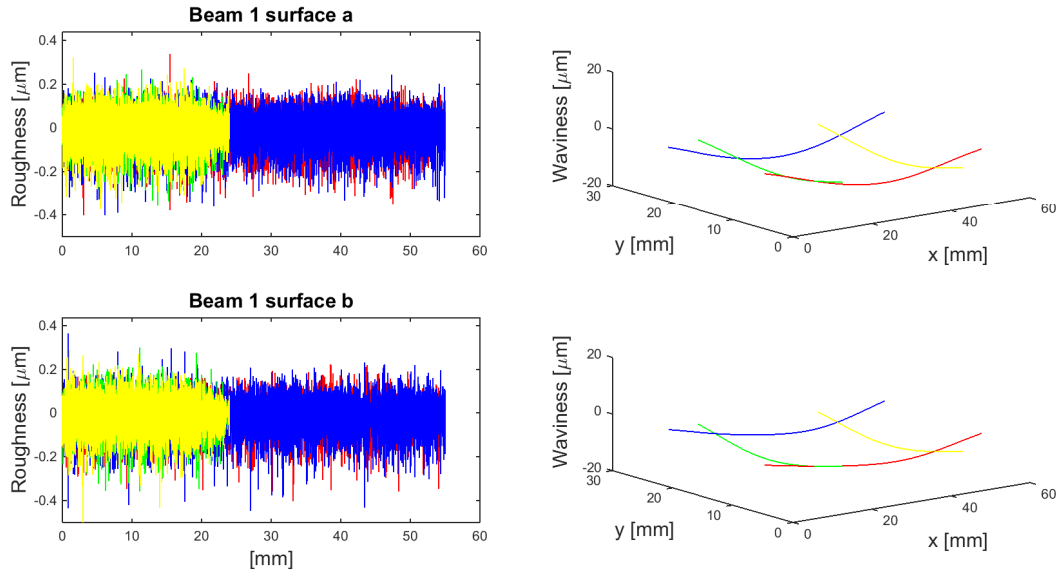


Figure 10: Roughness and waviness of the two surfaces of beam 1.

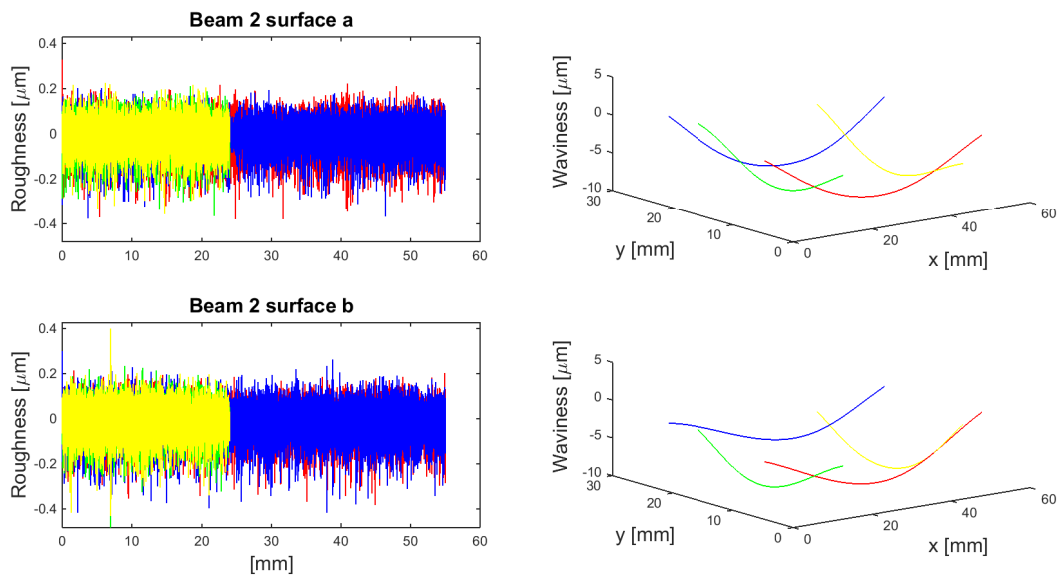


Figure 11: Roughness and waviness of the two surfaces of beam 2.

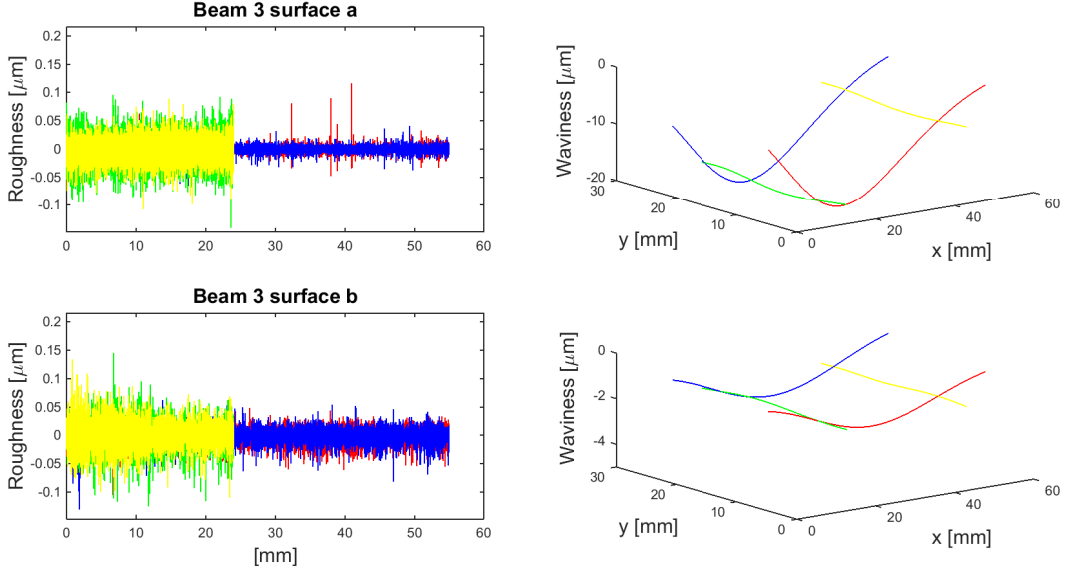


Figure 12: Roughness and waviness of the two surfaces of beam 3.

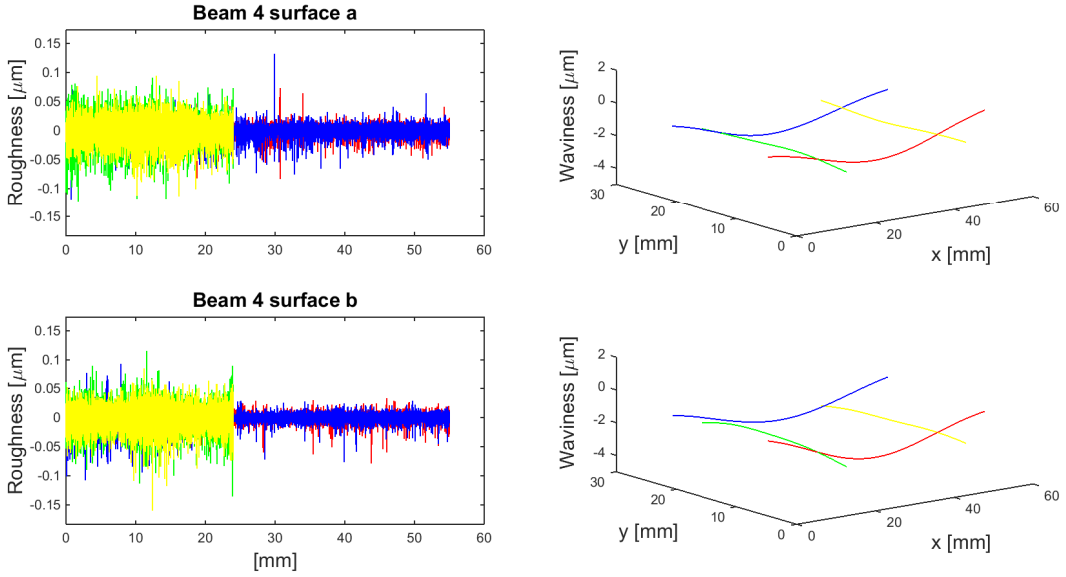


Figure 13: Roughness and waviness of the two surfaces of beam 4.

It can be seen that the waviness is similar for all surfaces within a few micrometers. In the surface of beam 3a is a small crack, which leads to the distorted result and the big drop in the waviness of the surface, as seen in Fig. 12. The roughness measurements provide some interesting results. Not only is the roughness different between beams with different surface treatments but there are also differences in the roughness values for measurements on the same surface for beams 3 – 6. Beams 1 and 2 are not treated and have therefore the roughest surfaces. The roughness is consistent in longitudinal and perpendicular direction. The polishing of beams 3 and 4 reduces the roughness, however, inconsistencies in the polishing process are causing different roughness values for the longitudinal and perpendicular direction. Beams 5 and 6 are polished even finer. This results in a further decrease of roughness. A similar effect to the one observed for the roughness of beam 3 and 4 can be seen on beam 5a. The roughness is different in longitudinal and perpendicular direction. In contrary to beam 3 and 4, for beam 5a the roughness in longitudinal direction is higher.

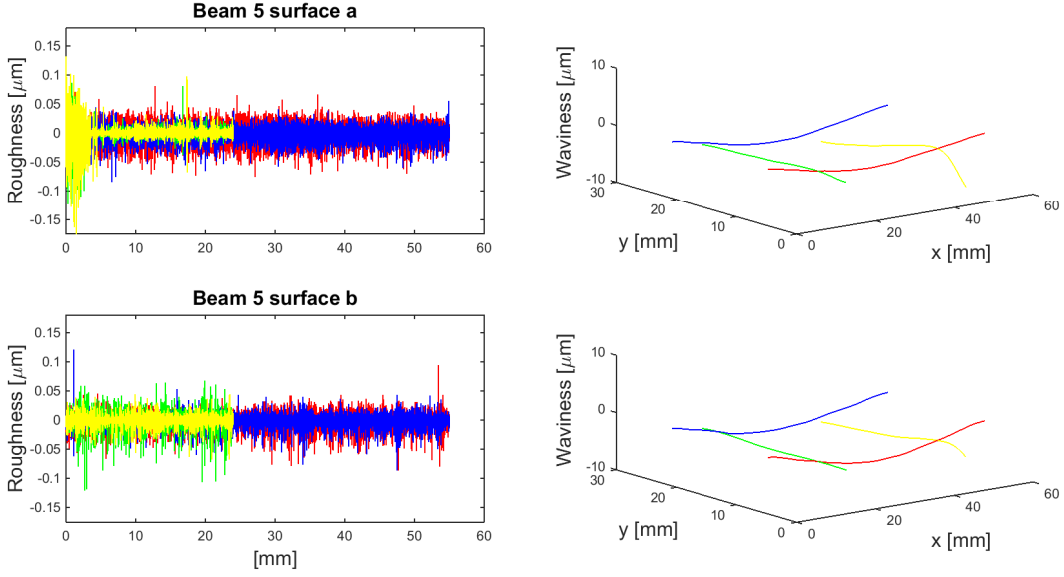


Figure 14: Roughness and waviness of the two surfaces of beam 5.

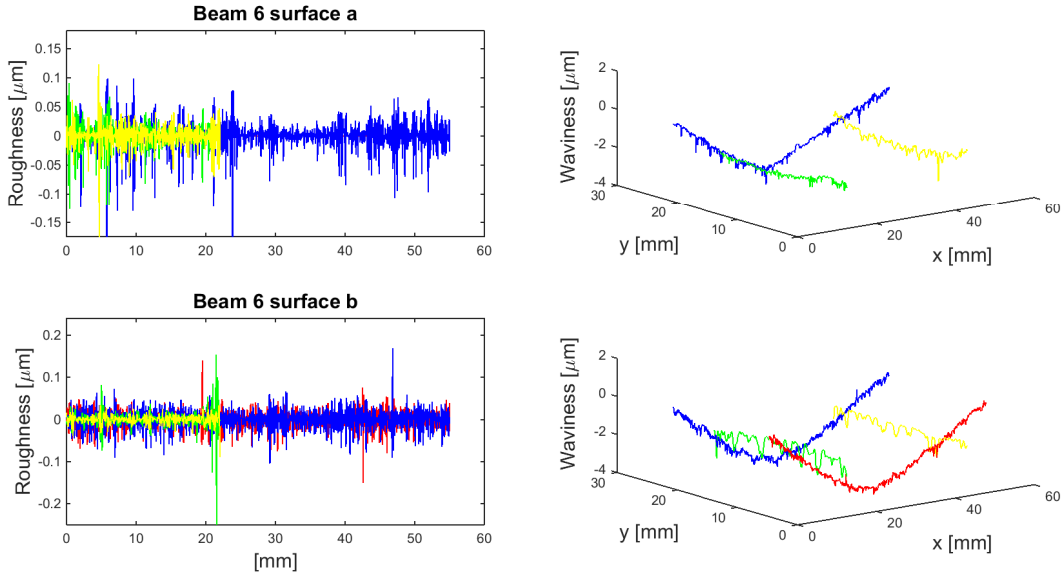


Figure 15: Roughness and waviness of the two surfaces of beam 6.

## 4 Joint Model Parameter Estimation

As stated in the Introduction, the objective of the present investigation was to collect joint response data appropriate to carry an ensuing identification yielding non-linear joint model parameters. This last effort is demonstrated here on the impact response data of section 3.1 and the parameters of the modal formulation of the Iwan model [2] are obtained.

In carrying out this identification, it is important to recognize the physical bounds on the parameters. In

particular, note that  $K_t, F_s, \beta$ , all belong to  $(0, \inf)$  while  $\chi$  is in the domain  $[-1, 0]$  with  $-1$  corresponding to a purely linear system.

## 4.1 Theory and Background

The four parameter Iwan [8], see section 2.3, was originally proposed to characterize a physical joint in terms of the force it carries and physical slip displacements it exhibits. However, it has recently been proposed as a modal representation of the joint(s) relating the modal force and corresponding generalized coordinate [2]. The same four parameters are used in both physical and modal representation but have different units.

The measurements used here are the time histories of the beam response (accelerations) to the impact at the accelerometer locations. These time histories exhibit non-linear effects at low time, when the system is in macro- or microslip, and becomes the response of a linear system as the time increases. The proposed analysis method of the acceleration data uses a combination of techniques [2]. The first step in the analysis is to decimate the time history to reduce the measurement error when the signal is close to zero and the system is not moving. After the signal is decimated, a band pass filter is applied to it to isolate the desired system resonance. This is an important step in the modal Iwan formulation to effectively reduce the system to a single degree of freedom model. Once the band pass filter is applied, the Hilbert transform is performed on the treated time history. This transform is utilized to get the frequency and damping of the signal as a function of amplitude which is the primary data used to determine the model Iwan joint parameters. The steps of the process are highlighted in the flowchart of Fig. 16.

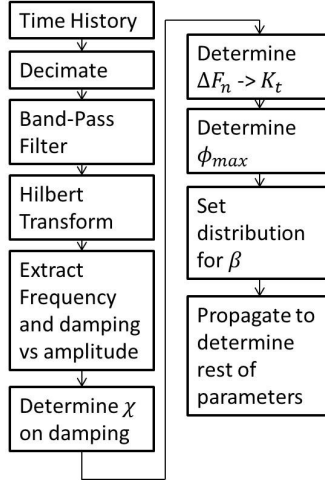


Figure 16: Non-linear Parameter Estimation Process

The results of this process are shown in Figs. 17-18 for beam 1 with a bolt torque of  $3Nm$ . It is seen that the frequency of the response decreases with increasing modal amplitude consistently with the previously observed softening behavior. In fact, these results match those obtained in the previous experiments reported in [1]. The damping plot, Fig. 18, exhibit three different regions: linear damping, microslip, and macroslip zones. In the linear range, i.e., for amplitudes below  $10^{-2}$ , the damping is constant and small, accordingly highly affected by the Hilbert transform noise. The microslip region extends from an amplitude of  $10^{-2}$  till  $7 * 10^{-2}$  and is characterized by a linear increase of the damping in a log-log plot. The slope of this line is related to  $\chi$  as will seen below. Finally, in the macroslip region, for amplitudes higher than  $7 * 10^{-2}$ , the damping is a quadratic function of amplitude. From 18, it is concluded that the joint experienced macroslip during the testing.

Consider next Figs. 19-20 which present frequency and damping vs. amplitude from the Hilbert transform for beam 1 with a bolt torque of  $15Nm$ . Comparing these figures with 17-18, it is first confirmed that the increase in torque renders the joint stiffer but also more linear, i.e., the linear range of the damping extends

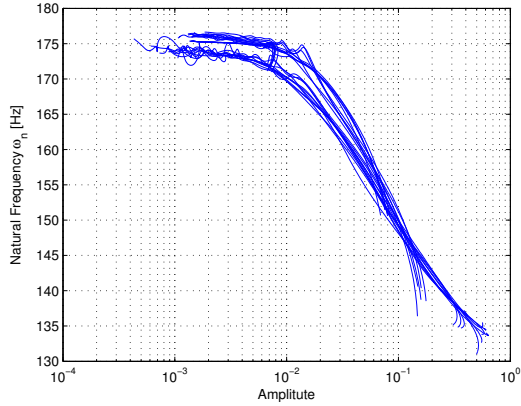


Figure 17: 3NM Torque Natural Frequency vs. Amplitude

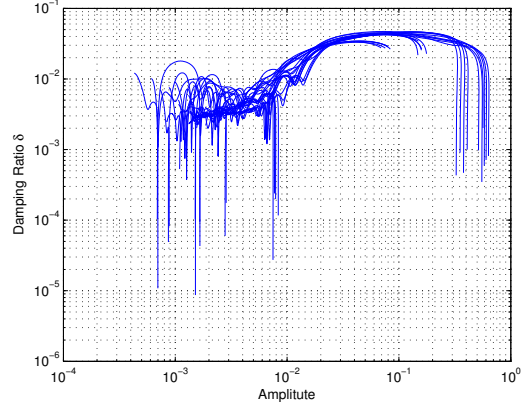


Figure 18: 3NM Torque Damping Ratio vs. Amplitude

further and macroslip does not appear to have occurred. Finally, note from Fig. 19 that the decrease in the natural frequency is linear with respect to the amplitude.

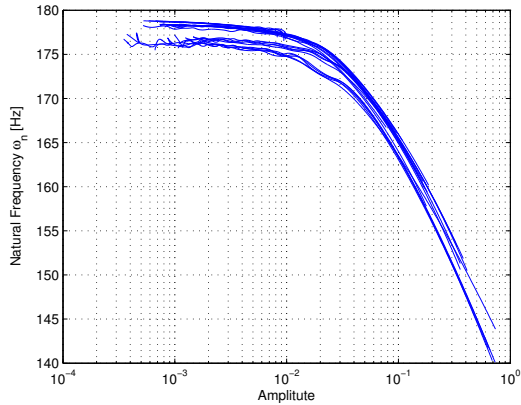


Figure 19: 15NM Torque Natural Frequency vs. Amplitude

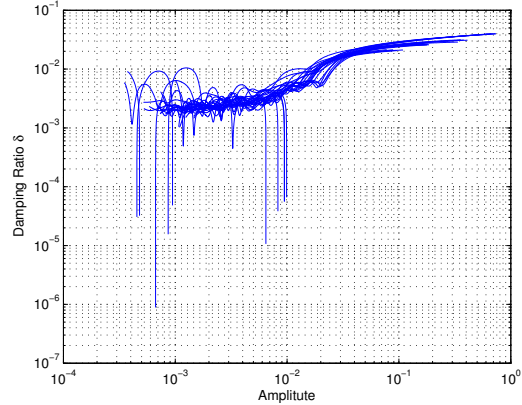


Figure 20: 15NM Torque Damping Ratio vs. Amplitude

Note in Figs. 17-20 that the multiple curves shown correspond to different repeats of the same condition. Their clustering shows the repeatability of the experimental techniques. Note as well the consistency of the frequency and damping vs. amplitudes curves obtained from high and low torque levels results suggesting the applicability of the Hilbert transform in a broad set of conditions.

## 4.2 Parameter Distributions

Three of the modal Iwan parameters can be determined from the frequency and damping vs. amplitudes curves shown above. The first such parameter is  $\chi$ . Specifically, it can be obtained from the slope of the damping vs. amplitude curve in the microslip regime [8] as

$$\chi = \text{slope} - 1. \quad (3)$$

The slope was determined by a simple linear least squares fit. The many repeats that were recorded can be used to obtain not only a typical value for  $\chi$  but also to estimate the variability (or uncertainty) of this parameter. With 25 data points, it is not possible to construct a probability density function using standard nonparametric methods (i.e., histograms) but given the range of  $\chi$ , i.e.,  $[-1, 0]$ , it is suggested here that it may be modeled by a Beta distribution. In order to chose a distribution for this value, a parametric approach is used since there is 25 data points that is unable to determine a full probability density function. The distribution chosen for this parameter is a beta distribution yielding the model

$$\chi \sim \beta(a, b) - 1, \quad (4)$$

where  $\beta(a, b)$  denotes a Beta distributed random variables with parameters  $a$  and  $b$  (referred to as hyperparameters).

The remaining two parameters of the modal Iwan model are determined from the frequency vs. amplitude curves. Specifically,  $\phi_{max}$  is the modal amplitude at which macroslip is expected to occur. This event triggers a rapid change of frequency and thus  $\phi_{max}$  would be determined from such a change. Figures 17 and 19 shows a fast but gradual change and thus the above condition to determine  $\phi_{max}$  must be accordingly amended. The zone of frequencies in which it varies rapidly is first identified as follows. Its lower limit is the frequency equal to 99% of the maximum frequency observed while the upper limit is 101% of the minimum frequency observed. The average of these frequencies is assumed to give the frequency at macroslip and thus  $\phi_{max}$  is read as the corresponding amplitude. Again, the multiple repeats allow the possibility for a probabilistic modeling of this parameter. As it is positive, a Gamma distribution was assumed as in [5] and fitted to the data.

The last experimentally determined parameter is the joint tangential stiffness  $K_T$ , it can be estimated similar to [2] as

$$K_T = \omega_{max}^2 - (\omega_{max} - \Delta\omega)^2, \quad (5)$$

where  $\omega_{max}$  is the maximum frequency in  $\frac{\text{radians}}{\text{sec}}$ , and  $\Delta\omega$  is the total frequency shift is the difference between the upper and lower limits of the zone of frequency change defined above. Since  $\Delta\omega$  uses the data from all impacts, only a single value of it can be determined. Thus, only a nominal value of  $K_T$  can be obtained in this manner, otherwise an exponential distribution would be selected as in [5] and fitted to the data. The selection of an exponential distribution utilizes that the stiffness can go to zero that corresponds to complete separation inside the lap joint. While this separation was not realized experimentally, a very small value of stiffness can be realized if the bolt torque is small and the impact is large enough. This outcome would result in complete separation of the beam, which is unable to happen due to the bolts in the joint. A small stiffness would correspond to the response of a test where pinning occurs but before the physical pinning happens.

With the experimental parameters determined, one parameter remains undetermined,  $\beta$ . The  $\beta$  parameter is bounded to be positive but is typically small. To fit the bounds and an expected value, a gamma distribution is given to the  $\beta$  parameter. The hyper-parameters of the  $\beta$  parameter distribution are chosen based on expert knowledge. The four parameters determined are in both the physical and the mathematical formulations of the Iwan model. Three of the parameters are in physical formulation with one in the mathematical formulation. The fourth physical parameter is the force at macroslip  $F_s$ . The macroslip force can be determined via

$$F_s = \frac{\phi_{max} K_T (\beta + \frac{\chi+1}{\chi+2})}{1 + \beta}. \quad (6)$$

Performing a Monte-Carlo analysis yields the distribution of the macroslip force. This method is done for the beam one with a bolt torque of  $3Nm$ . The distributions of this Monte-Carlo analysis are shown in Figures 21-24. The output distribution fits a gamma distribution in both shape and bounds and is shown in Figure 24.

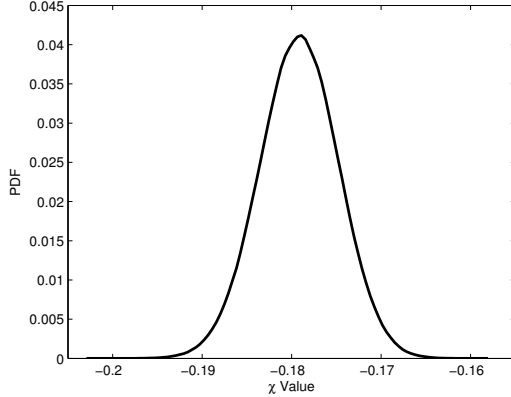


Figure 21:  $\chi$  Distribution

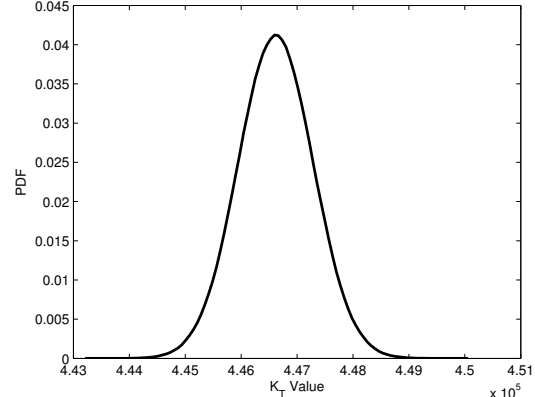


Figure 22:  $K_T$  Distribution

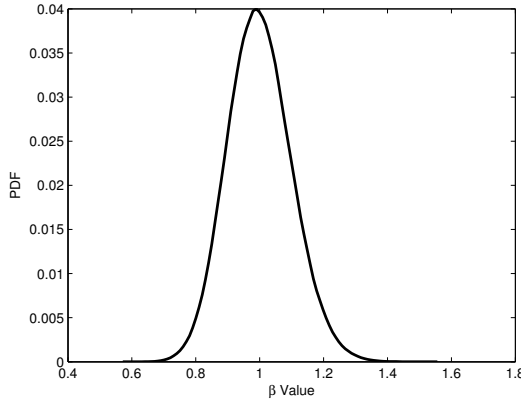


Figure 23:  $\beta$  Distribution

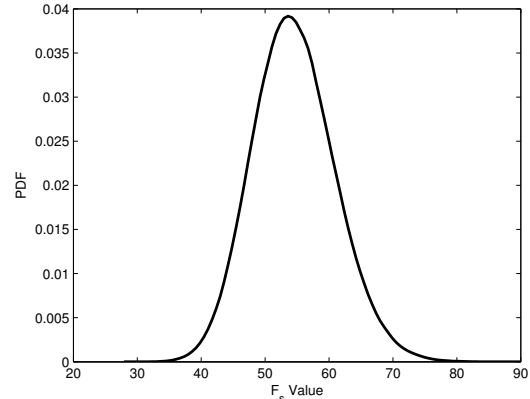


Figure 24:  $F_s$  Distribution

The distribution of the parameters look similar to the distribution at different torque values. The analysis is also run on beam one with a bolt torque of  $5Nm$ , which is similar to the previous analysis but still show the changes due to a change in bolt torque. The values for the mean and standard deviation of each parameter is shown in Table 1. An important relationships that is expected is with the increase in torque, the joint becomes stiffer and more linear. This is denoted by the increase in tangential stiffness and slip force. The linear relation is seen in  $\chi$ , which is closer to  $-1$  that corresponds to a linear system.

Table 1: Parameters for Beam 1 with 3 and 5 Nm Torque

Parameter	3Nm torque		5Nm torque	
	Mean	StandardDeviation	Mean	StandardDeviation
$\phi_{max}$	$1.68 * 10^{-4}$	$1.955 * 10^{-5}$	$1.62 * 10^{-4}$	$1.01 * 10^{-5}$
$K_T$	$4.47 * 10^5$	$\sim$	$6.048 * 10^5$	$\sim$
$\chi$	-0.179	.0044	-0.480	0.062
$F_s$	54.5	6.42	65.8	4.60

## 5 Plasticity Effects

The impact testing effort began by completing a series of low level impact tests on the beams which behave almost entirely in the linear range, resulting in a first natural frequency around 180 Hz. Once the low level impact tests were completed, higher level ones were performed that showed not only microslip but with definite macroslip as well. In those tests, the natural frequency dropped to around 130 Hz.

Given the magnitude of the drop in frequency, it was decided to repeat low impact level tests to confirm that the large loads had not modified the joint. These tests however *did not* recover the 180Hz frequency but rather around 160 Hz. There was thus a permanent loss of stiffness leading to a 20 Hz frequency drop. Figure 25 shows frequency response functions before and after the high level impacts and the frequency shift.

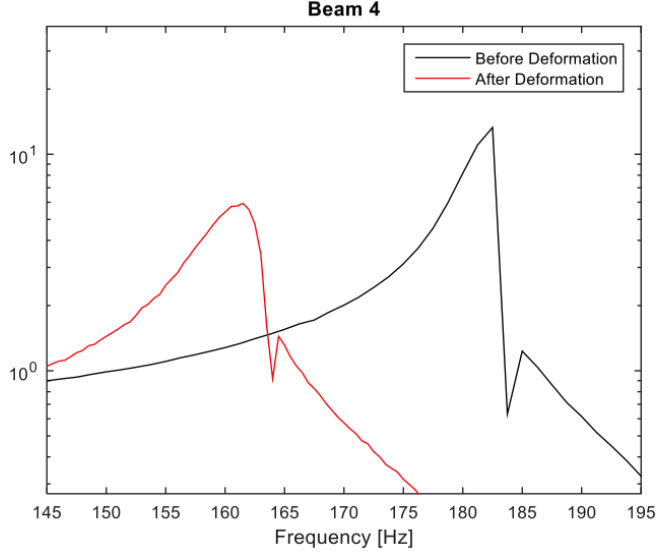


Figure 25: Permanent Frequency Shift - Beam 4

To understand the reasons for the change in joint behavior, disassembly and reassembly was first performed to check for loose connections but the natural frequency remained in the neighborhood of 160 Hz. Next, a close inspection of the surfaces was undertaken to check for defects and this effort revealed the pair of markings seen on Fig. 26. It is construed that plastic deformations have occurred in that zone thus irreversibly changing the joint.

Likely related to the damage of Fig. 26, an unusual behavior of beams 3 and 4 was observed after the high level impacts were completed. Specifically, it was found that their natural frequencies *decrease* with increasing torque level at the contrary of both physical expectations (see above for discussion) and findings on other beams, compare Figs. 28 and 27. The mechanics of this observation is not clear that it appears to be an interaction between the stress induced by the bolts and the residual stress distribution resulting from the macroslip event.

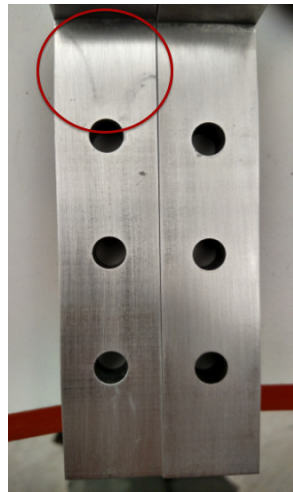


Figure 26: Visible Damage in Beam 4

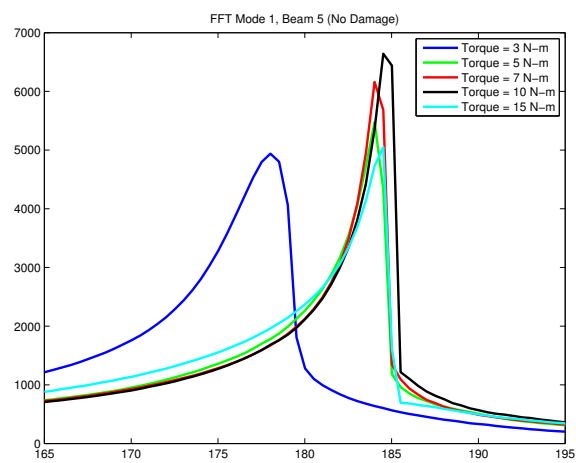


Figure 27: Frequency Shift Increase Due to Increased Torque - Beam 5 (No Abnormality)

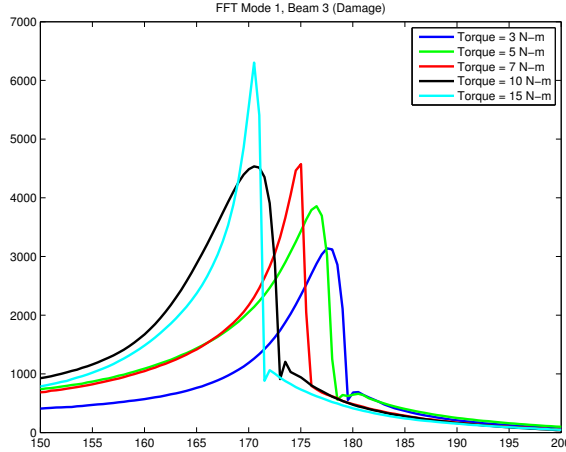


Figure 28: Frequency Shift Decrease Due to Increased Torque - Beam 3 (Abnormality)

## 6 Conclusions

The present investigation focused on generating, analyzing, and processing free responses, acceleration data more specifically, of the Brake-Reuß beam to assess its potential to determine the parameters of a modal Iwan model of the lap joint. Consideration was also given to developing uncertain models of these parameters.

This effort has demonstrated the application of the Hilbert transform applied as follows on the acceleration data. The time history is first decimated to reduce the measurement error, a bandpass filter is then applied to the signal to isolate a signal resonance, and finally the Hilbert transform is performed on the treated time history. The result of this process are frequency and damping vs. amplitude curves which permit the identification of the parameters of a modal Iwan model as demonstrated. These curves also show the effect of the bolt torque on the joint behavior, i.e., increase in natural frequency, linear limit, and macroslip threshold.

Macroslip is shown to have occurred in some of the tests and it is concluded from ensuing testing that this event changed the nature of the jointed beams. Specifically, the linear natural frequency (observed under very low level impact test) shifted permanently by 20Hz and, in one case, the linear natural frequency was observed to decrease with increasing bolt torque level in opposition to other beams and physical expectations. An analysis of the joint surface strongly suggest that a significant plastic zone developed during the macroslip phase which induced the above unusual behaviors. This finding suggests that the testing process should be done in increasing impact magnitude to capture the linear zone, then microslip, and finally macroslip with the testing stopped when the linear natural frequency is no longer recovered after a test.

Detailed measurements of the profile of the joint surface was also carried out for the beams tested. This data will be used in the near future with the impact test analyses to develop correlations between state of surface, torque levels, impact levels, and the corresponding modal Iwan parameters to better understand the effects of these conditions on the joint behavior.

## References

- [1] M.R.W. Brake, P. Reuss, C.W. Schwingshackl, L. Salles, M.E. Negus, D.E. Peebles, R.L. Mayes, M.S. Bilbao-Ludena, J.C. Bonney, S. Catalfamo, C. Gastaldi, J. Gross, R.M. Lacayo, B.A. Robertson, S. Smith, C. Swacek, and M. Tiedemann. The 2014 sandia nonlinear mechanics and dynamics summer research institute. Technical Report SAND2015-1876, Sandia National Laboratories Livermore, CA; Sandia National Laboratories (SNL-NM), Albuquerque, NM (United States), 2015.
- [2] B. Deaner, M.S. Allen, M.J. Starr, D.J. Segalman, and H. Sumali. Application of viscous and iwan modal damping models to experimental measurements from bolted structures. *ASME Journal of Vibration and Acoustics*, 137, 2015.
- [3] L. Gaul and R. Nitsche. The role of friction in mechanical joints. *Appl Mech Rev*, 54(2):93–109, 2001.
- [4] G. M. Jenkins. Analysis of the stress-strain relationships in reactor grade graphite. *Brit. J. Appl. Phys.*, 13:30–32, 1962.
- [5] M.P. Mignolet, P. Song, and X.Q. Wang. A stochastic iwan-type model for joint behavior variability modeling. *Journal of Sound and Vibration*, 349:189–298, 2015.
- [6] B. A. Robertson, M. S. Bonney, C. Gastaldi, and M. R. W. Brake. Quantifying epistemic and aleatoric uncertainty in the ampair 600 wind turbine. *Proceedings of the 33rd International Modal Analysis Conference (IMAC XXXIII)*, 2015.
- [7] D. J. Segalman, D. L. Gregory, M. J. Starr, B. R. Resor, M. D. Jew, J. P. Lauffer, and N. M. Ames. Handbook on dynamics of jointed structures. Technical Report SAND2009-4164, Sandia National Laboratories, Albuquerque, NM, 2009.
- [8] D.J. Segalman and M.J. Star. A four-parameter iwan model for lap-type joints. *ASME J. Appl. Mech.*, 72:752–760, 2005.
- [9] S. Smith, J.C. Bilbao-Ludena, S. Catalfamo, M. R. W. Brake, P. Reuss, and C. W. Schwingshackl. The effects of boundary conditions, measurement techniques, and excitation type on measurements of the properties of mechanial joints. *Proceedings of the 33rd International Modal Analysis Conference (IMAC XXXIII)*, 2015.